Methyl Transfer in Glycine *N*-Methyltransferase. A Theoretical Study

Polina Velichkova and Fahmi Himo*

Theoretical Chemistry, Department of Biotechnology, Royal Institute of Technology, Albanova University Center, SE-106 91 Stockholm, Sweden

Received: December 13, 2004; In Final Form: February 15, 2005

Density functional theory calculations using the hybrid functional B3LYP have been performed to study the methyl transfer step in glycine *N*-methyltransferase (GNMT). This enzyme catalyzes the *S*-adenosyl-L-methionine (SAM)-dependent methylation of glycine to form sarcosine. The starting point for the calculations is the recent X-ray crystal structure of GNMT complexed with SAM and acetate. Several quantum chemical models with different sizes, employing up to 98 atoms, were used. The calculations demonstrate that the suggested mechanism, where the methyl group is transferred in a single S_N2 step, is thermodynamically plausible. By adding or eliminating various groups at the active site, it was furthermore demonstrated that hydrogen bonds to the amino group of the glycine substrate lower the reaction barrier, while hydrogen bonds to the carboxylate group raise the barrier.

I. Introduction

Glycine *N*-methyltransferase (GNMT) catalyzes the transfer of a methyl group from *S*-adenosylmethionine (SAM) to glycine, resulting in the formation of sarcosine (*N*-methylglycine) and *S*-adenosylhomocysteine (SAH), Scheme 1. GNMT is abundant in liver, where it makes up 1−3% of the soluble protein in the cytosol.[1] The sarcosine has no known physiological function, and it is converted back to glycine by sarcosine dehydrogenase.[2] This, together with the fact that GNMT, unlike most SAM-dependent methyltransferases, is very little inhibited by the product SAH, has led researchers to suggest that the role of GNMT is to regulate the cellular SAM/SAH ratio,[3] which is important for the activity of other methyltransferases in the cell.[4]

The crystal structure of GNMT was first determined in 1996 by Fu et al.[5] Crystal structures of substrate-free[6] and mutated (R175K)[7] GNMT have also been reported. More recently, a mechanistically more interesting structure of GNMT was solved, namely, in complex with SAM and an acetate molecule.[8] In Figure 1, the main features of the active site of this structure are displayed.

The guanidino group of Arg175 forms a pair of hydrogen bonds with the carboxylate group of the acetate, and also the residues Tyr33, Tyr220, Asn138, and Gly137 help in orienting the acetate. When a glycine is modeled into the active site by adding an amino group to the acetate, it is seen that the lone pair of the nitrogen is pointing toward the C_E of SAM.[8]

On the basis of this GNMT:(SAM + acetate) structure, and previous biochemical and spectroscopic work, the following mechanism has been proposed for GNMT.[8] The reaction starts with the binding of SAM and the glycine substrates, in this strict order. The glycine binds in such a way that the lone pair of the amino nitrogen is directed toward the C_E methyl carbon of SAM. Then, a single S_N2 methyl transfer step occurs. The charge−dipole interaction between S_D of SAM and O_H of Tyr21 is proposed to polarize the S−C bond and facilitate the S_N2 reaction. Finally, the methylated glycine is now less favorably bound in the active site because of its positive charge and is therefore released.

SCHEME 1: Reaction Catalyzed by GNMT

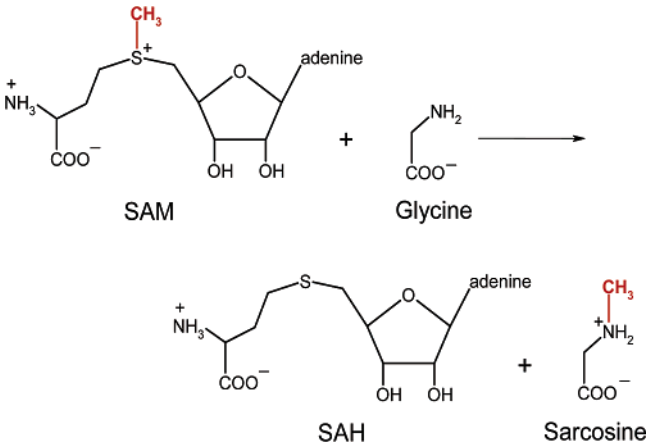

In the present study, we have explored the energetics of the methyl transfer step of this mechanism employing quantum chemical models of different sizes, based on the crystal structure of Takata et al.[8] We use the hybrid density functional theory (DFT) method B3LYP,[9] which has been extensively used to study enzyme mechanisms of this kind in recent years.[10]

II. Computational Details

All geometries and energies presented in the present study are computed using the B3LYP[9] density functional theory method as implemented in the Gaussian03 program package.[11] Geometry optimizations were performed using the 6-31G(d,p) basis set. On the basis of these geometries, single-point calculations with the larger basis set 6-311+G(2d,2p) were done to obtain more accurate energies. Solvation energies were added as single-point calculations using the conductor-like solvation model COSMO[12] at the B3LYP/6-31G(d,p) level. In this model, a cavity around the system is surrounded by a polarizable dielectric continuum. The dielectric constant chosen is $\epsilon = 4$, which is the standard value used to model the protein surround-

* To whom correspondence should be addressed. E-mail: himo@theochem.kth.se.

10.1021/jp0443254 CCC: $30.25
Published on Web 04/02/2005

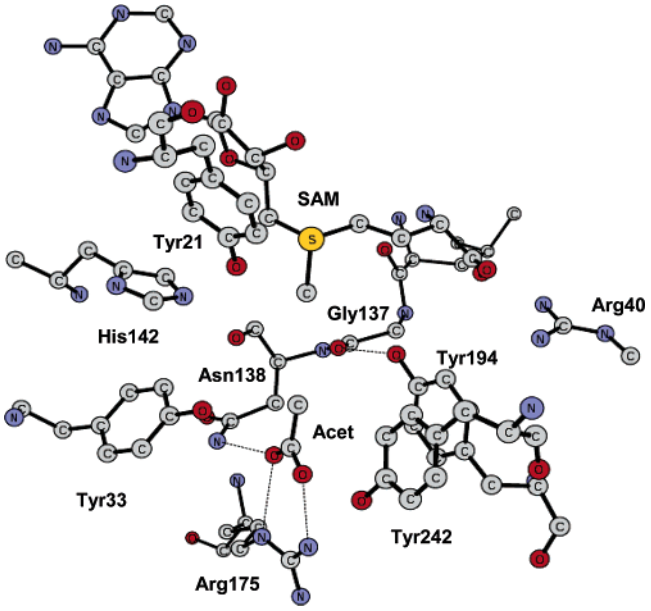

Figure 1. X-ray crystal structure of the active site of GNMT. Reprinted from ref 8. Copyright 2003 American Chemical Society.

ings. Hessians were calculated at the B3LYP/6-31G(d,p) level to confirm the nature of the stationary points, with no negative eigenvalues for minima and only one negative eigenvalue for transition states. The Hessians were also used to calculate zero-point vibrational effects. For the largest model consisting of 98 atoms, the Hessians were not calculated. Instead, the zero-point effects were estimated as an average of the zero-point effects of the smaller models. This is a good approximation, considering that zero-point effects vary very little among the models (less than 1 kcal/mol for the transition states). As will be discussed below, some centers were kept fixed to their X-ray positions. This procedure gives rise to a few small imaginary frequencies, typically on the order of 10 cm^{-1}. These frequencies do not contribute significantly to the zero-point energies and can thus be tolerated. The energies reported in the present paper include both solvation and zero-point effects.

III. Results and Discussion

In the present study, several quantum chemical models with different sizes, ranging from 22 atoms up to 98 atoms, have been used to study the methyl transfer step in GNMT. We start by discussing the results from the largest, and hence most reliable, model and then move to discuss the smaller models that were designed to investigate the role of the different residues at the active site of GNMT.

In the largest model, the following groups are included (see Figure 2): (1) A model of SAM, which is truncated two carbons away in each direction from the sulfur center. This is sufficient to model the properties of the S_D-C_E bond and to grant some flexibility to the SAM model. The S−C bond strength of this model is calculated to be 115.8 kcal/mol (gas phase, no zero point), only 1.0 kcal/mol lower than the S−C bond strength of the full SAM cofactor (calculated to be 116.8 kcal/mol). On the contrary, truncating only one carbon away yields an S−C bond strength of 111.1 kcal/mol, 5.7 kcal/mol off the full SAM value. (2) The glycine substrate, which was modeled on the basis of the structure of the acetate, to which an amino group was added. (3) The side chain of Arg175, because this group forms strong hydrogen bonds to the carboxylate of glycine and is hence essential to bind the substrate and stabilize its charge. (4) The phenol group of Tyr21, to test the proposal that this group polarizes the S−C bond of SAM. (5) Parts of Gly137 and Asn138, as these groups are found to form hydrogen bonds to both the amino and the carboxylate groups of the glycine substrate. (6) The phenol group of Tyr194, since this group forms hydrogen bonds to both the glycine substrate and Gly137.

The coordinates were taken from the recent GNMT:(SAM + acetate) X-ray crystal structure[8] (PDB code 1NBH), and hydrogen atoms were added manually. To keep the various groups in place to as much as possible resemble the crystal structure, certain atoms, typically where the truncation is done, were kept frozen to their X-ray positions. These atoms are indicated by arrows in the figures.

The optimized structure of the reactant species is shown in Figure 2A. Overall, this structure shows a quite high resemblance to the crystal structure. We notice that the protein environment around the substrate, mainly the hydrogen-bonding network (to Arg175, Gly137, and Asn138), helps in orienting the glycine such that there is a nearly straight line between the sulfur center of SAM, the methyl group to be transferred, and the nitrogen of the glycine substrate. The distance between C_E and N in this model is calculated to be 3.09 Å.

We find that the methyl group is transferred as a cation in a single S_N2-type step, which involves inversion of the methyl. The structures of the optimized transition state (TS) and product are displayed in parts B and C of Figure 2, respectively. The barrier is calculated to be 15.0 kcal/mol, and the reaction is

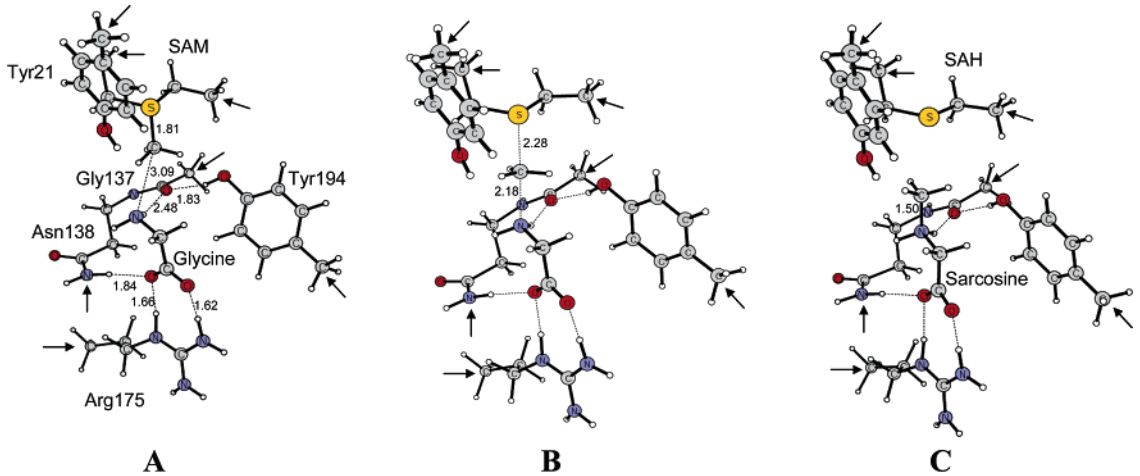

Figure 2. Optimized structures of the (A) reactant, (B) transition state, and (C) product of the largest model of GNMT used in the present study. Distances are in angstroms. Arrows indicate atoms that are fixed to their X-ray positions.

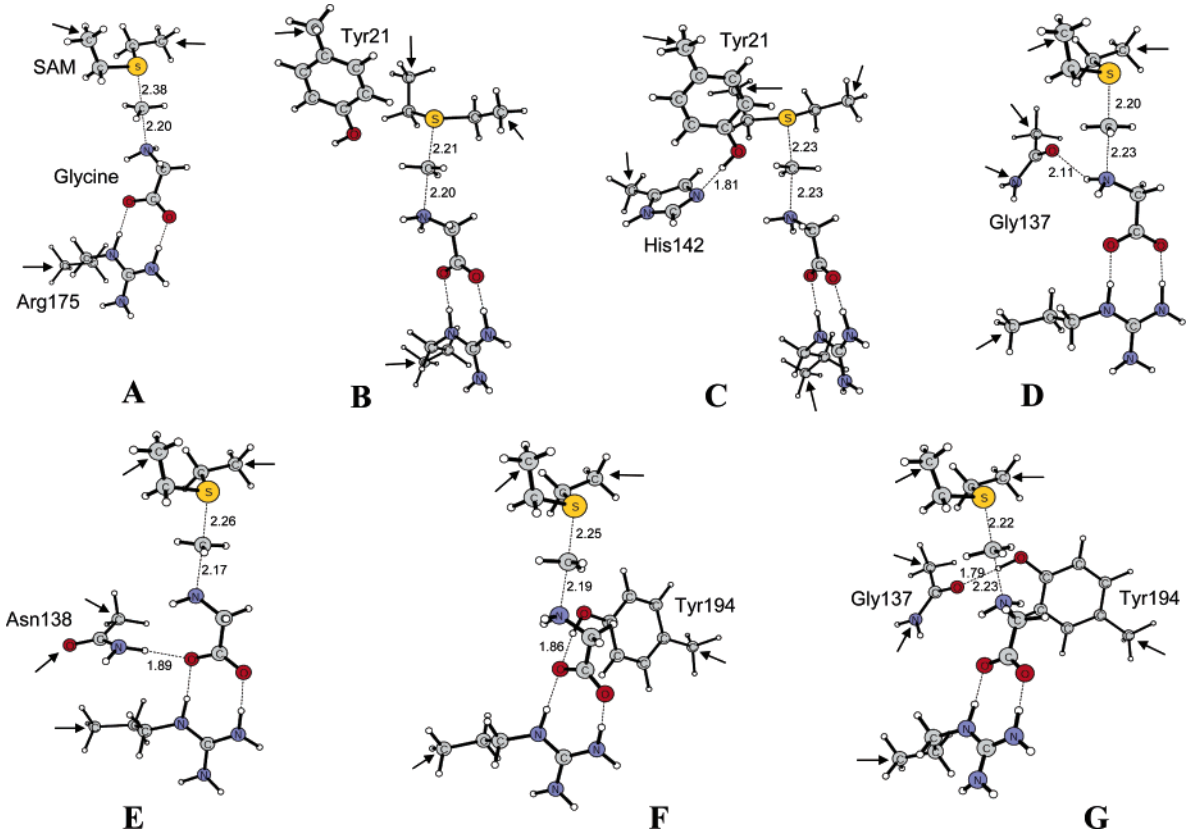

Figure 3. Optimized transition-state structures for models A−G.

TABLE 1: Calculated Barriers and Reaction Energies (kcal/mol) for the Different Models Used[a]

model	parts included	barrier	reaction energy	S_D-C_E	C_E-N
A	SAM + glycine + Arg175	11.2	−20.1	2.34	2.20
B	A + Tyr21	13.5	−16.8	2.21	2.20
C	A + Tyr21 + His142	11.4	−21.2	2.23	2.23
D	A + Gly137	9.9	−24.8	2.20	2.23
E	A + Asn138	15.1	−12.6	2.26	2.17
F	A + Tyr194	17.5	−14.5	2.25	2.19
G	A + Tyr194 + Gly137	10.5	−16.6	2.22	2.23
largest	A + Tyr21 + Gly137 + Asn138 + Tyr194	15.0	−14.1	2.28	2.18

[a] S_D-C_E and C_E-N bond distances (Å) at the transition states are also included (see Figures 2 and 3).

found to be exergonic by 14.1 kcal/mol. At the TS, the critical S_D-C_E and C_E-N bond distances are 2.28 and 2.18 Å, respectively. These energies show that the postulated one-step S_N2 methyl transfer from SAM to glycine is indeed energetically feasible.

Having established this, we now focus on the effects of the various groups in the active site. To do this, we use a small model consisting of SAM, the glycine substrate, and the side chain of Arg175 (called model A, Figure 3A), and add the other residues one at a time. This way, one is able to isolate the contribution of each group. The energetic results are summarized in Table 1, and the optimized transition state structures are shown in Figure 3.

Model A has a barrier of 11.2 kcal/mol and is exothermic by 20.1 kcal/mol. Adding the phenol group of Tyr21 to this model results in a slight increase of the barrier, to 13.5 kcal/mol, and a decrease of the exothermicity, to 16.8 kcal/mol (model B in Table 1 and Figure 3B). When both Tyr21 and the imidazole ring of His142 are added (model C, Figure 3C) the barrier is found to be almost identical to that of model A, 11.4 kcal/mol. These results speak against the suggestion that Tyr21 polarizes the S−C bond to cause a decrease in the barrier.[8] As also seen for the largest model discussed above (Figure 2), the phenolic proton of Tyr21 was found to point away from SAM, despite attempts to make it point toward the sulfur center.

Adding the peptide bond of Gly137, which forms a hydrogen bond to the amino group of the substrate (model D, Figure 3D), results in a decrease of the barrier by 1.2 kcal/mol to 9.9 kcal/mol. The hydrogen bond to the carbonyl moiety of Gly137 makes the nitrogen center of the substrate slightly more negative, which makes the transfer of the positively charged methyl group slightly easier. Mulliken population analysis confirms this picture: in model A the nitrogen bears a charge of −0.48, while in model C the charge is −0.51. At the transition state, the difference is larger, from −0.29 to −0.35.

In contrast, adding the side chain of Asn138, which forms a hydrogen bond to the carboxylate moiety of the substrate, will make the substrate slightly less negative, which in turn would lead to a higher barrier, calculated to be 15.1 kcal/mol (model E, Figure 3E). The Mulliken charge on the nitrogen is now −0.44 in the reactant species and −0.26 at the transition state.

Adding the Tyr194 residue to model A leads to a dramatic increase of the barrier, from 11.2 to 17.5 kcal/mol (model F, Figure 3F). This is easily explained if we note that the phenolic

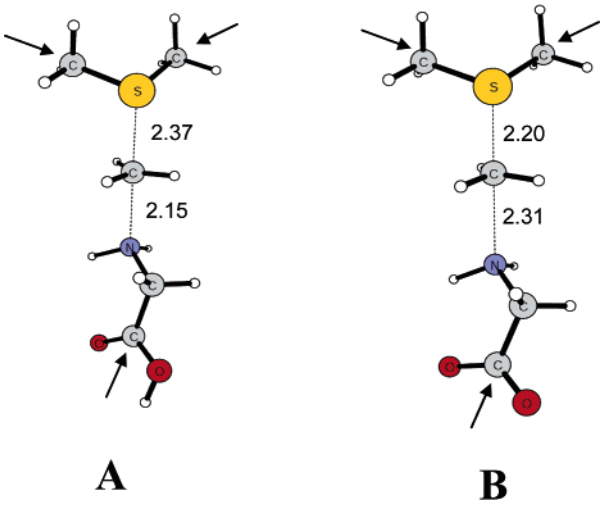

Figure 4. Optimized transition-state structures for the small protonated model (A) and the small anionic model (B). Note that the geometry optimization for the anionic system was performed in a dielectric medium.

proton forms a hydrogen bond to the nitrogen atom of the substrate in the reactant species. This hydrogen bond will be lost when the methyl is transferred to the nitrogen, resulting in the barrier increase. On the other hand, if both Tyr194 and the peptide bond of Gly137 are added at the same time (model G, Figure 3G), the tyrosine will form a hydrogen bond to the carbonyl of the glycine instead and the barrier will be lowered to 10.5 kcal/mol.

In Table 1, we have also listed the S_D-C_E and C_E-N bond distances at the transition states of the different models. We notice that the variation is quite small. This confirms our general experience that the local structure of a transition state is to a large extent independent of the size of the model. Using this experience, we often perform the tedious work of finding the TS for as small a model as possible and then transfer the information (bond distances and angles) to the large model, which makes it then much easier to locate the transition state. Note that although the local structure of the TS does not change much, the energies can differ a lot.

Finally, just for comparison, we also tried a very small model in which the arginine group hydrogen bonding to the glycine carboxylate was removed and the carboxylate moiety was protonated, making the substrate charge neutral. The SAM model was truncated only one carbon away from the sulfur center. It turns out that this model works exceptionally well. The barrier is calculated to be 16.6 kcal/mol (cf. 15.0 kcal/mol obtained for the largest model), and the S−C and C−N distances at the transition state are 2.37 and 2.15 Å, respectively, quite similar to those of the large model (2.28 and 2.18 Å, respectively); see the TS structure in Figure 4A.

When the carboxylate was left negatively charged and the Arg group was removed, the reaction proceeded without a barrier, when the calculations were done in the gas phase. Performing the optimization in solution (PCM model with $\epsilon = 4$), we could locate a transition state, shown in Figure 4B. Considering that a positively charged group is transferred to a negatively charged one, it is not surprising that the barrier is quite low, only 5.6 kcal/mol, and the transition state is quite early compared to those of the neutral model. The S−C distance is shorter (2.20 Å), and the C−N distance is longer (2.31 Å).

IV. Conclusions

We have in the present study used quantum cluster models of different sizes to investigate the methyl transfer reaction step in glycine *N*-methyltransferase. The models were based on the X-ray structure of Takata et al.[8] and consist of up to 98 atoms. The calculations have confirmed that the methyl transfer step occurs in a single S_N2 step. The calculated barrier using the largest model is 15.0 kcal/mol, and the reaction energy is −14.1 kcal/mol. By adding or eliminating various groups at the active site, we showed that hydrogen bonds to the amino group of the substrate lower the reaction barrier, whereas hydrogen bonds to the carboxylate group of the substrate raise the barrier. The suggested role of Tyr21 in polarizing the S−C bond of *S*-adenosyl-L-methionine, making the methyl transfer more facile, could not be confirmed.

Acknowledgment. We gratefully acknowledge financial help from The Swedish Research Council, The Wenner-Gren Foundations, The Carl Trygger Foundation, and The Magn Bergvall Foundation. We also thank the NSC for computer time.

References and Notes

(1) Heady, J. E.; Kerr, S. J. *J. Biol. Chem.* **1973**, *248*, 69.
(2) Wittwe, A. J.; Wagner, C. *J. Biol. Chem.* **1981**, *256*, 4102.
(3) Ogawa, H.; Fujioka, M. *J. Biol. Chem.* **1982**, *257*, 3447.
(4) Kerr, S. J.; Heady, J. E. *Adv. Enzyme Regul.* **1974**, *12*, 103.
(5) Fu, Z.; Hu, Y.; Konishi, K.; Takata, Y.; Ogawa, H.; Gomi, T.; Fujioka, M.; Takusagawa, F. *Biochemistry* **1996**, *35*, 11985.
(6) Pattanayek, P.; Newcomer, M. E.; Wagner, C. *Protein Sci.* **1998**, *7*, 1326.
(7) Huang, Y.; Komoto, J.; Konishi, K.; Takata, Y.; Ogawa, H.; Gomi, T.; Fujioka, M.; Takusagawa, F. *J. Mol. Biol.* **2000**, *298*, 149.
(8) Takata, Y.; Huang, Y.; Komoto, J.; Yamada, T.; Konishi, K.; Ogawa, H.; Gomi, T.; Fujioka, M.; Takusagawa, F. *Biochemistry* **2003**, *42*, 8394.
(9) (a) Lee, C.; Yang, W.; Parr, R. G. *Phys. Rev.* **1988**, *B37*, 785. (b) Becke, A. D. *Phys. Rev.* **1988**, *A38*, 3098. (c) Becke, A. D. *J. Chem. Phys.* **1992**, *96*, 2155. (d) Becke, A. D. *J. Chem. Phys.* **1992**, *97*, 9173. (e) Becke A. D. *J. Chem. Phys.* **1993**, *98*, 5648.
(10) (a) Siegbahn, P. E. M.; Blomberg, M. R. A. *J. Phys. Chem. B* **2001**, *105*, 9375. (b) Siegbahn, P. E. M. *Q. Rev. Biophys.* **2003**, *36*, 91. (c) Himo, F.; Siegbahn, P. E. M. *Chem. Rev.* **2003**, *103*, 2421.
(11) Gaussian 03: Frisch, M. J.; Trucks, G. W.; Schlegel, H. B.; Scuseria, G. E.; Robb, M. A.; Cheeseman, J. R.; Montgomery, J. A., Jr.; Vreven, T.; Kudin, K. N.; Burant, J. C.; Millam, J. M.; Iyengar, S. S.; Tomasi, J.; Barone, V.; Mennucci, B.; Cossi, M.; Scalmani, G.; Rega, N.; Petersson, G. A.; Nakatsuji, H.; Hada, M.; Ehara, M.; Toyota, K.; Fukuda, R.; Hasegawa, J.; Ishida, M.; Nakajima, T.; Honda, Y.; Kitao, O.; Nakai, H.; Klene, M.; Li, X.; Knox, J. E.; Hratchian, H. P.; Cross, J. B.; Bakken, V.; Adamo, C.; Jaramillo, J.; Gomperts, R.; Stratmann, R. E.; Yazyev, O.; Austin, A. J.; Cammi, R.; Pomelli, C.; Ochterski, J. W.; Ayala, P. Y.; Morokuma, K.; Voth, G. A.; Salvador, P.; Dannenberg, J. J.; Zakrzewski, V. G.; Dapprich, S.; Daniels, A. D.; Strain, M. C.; Farkas, O.; Malick, D. K.; Rabuck, A. D.; Raghavachari, K.; Foresman, J. B.; Ortiz, J. V.; Cui, Q.; Baboul, A. G.; Clifford, S.; Cioslowski, J.; Stefanov, B. B.; Liu, G.; Liashenko, A.; Piskorz, P.; Komaromi, I.; Martin, R. L.; Fox, D. J.; Keith, T.; Al-Laham, M. A.; Peng, C. Y.; Nanayakkara, A.; Challacombe, M.; Gill, P. M. W.; Johnson, B.; Chen, W.; Wong, M. W.; Gonzalez, C.; and Pople, J. A., Gaussian, Inc., Wallingford, CT, 2004.
(12) (a) Cammi, R.; Mennucci, B.; Tomasi, J. *J. Phys. Chem. A* **1999**, *103*, 9100. (b) Cammi, R.; Mennucci, B.; Tomasi, J. *J. Phys. Chem. A* **2000**, *104*, 5631. (c) Cossi, M.; Rega, N.; Scalmani, G.; Barone, V. *J. Chem. Phys.* **2001**, *114*, 5691. (d) Cossi, M.; Scalmani, G.; Rega, N.; Barone, V. *J. Chem. Phys.* **2002**, *117*, 43.